Title

CREEP AND DENSIFICATION DURING SINTERING OF GLASS POWDER COMPACTS: I. EFFECTS OF APPLIED STRESS AND TEMPERATURE

Authors

Rahaman, M.N.
Jonghe, L.C. De

Publication Date

1985-12-01

Lawrence Berkeley Laboratory
UNIVERSITY OF CALIFORNIA

Materials & Molecular Research Division

Submitted to Journal of the American Ceramic Society

CREEP AND DENSIFICATION DURING SINTERING OF GLASS POWDER COMPACTS: I. EFFECTS OF APPLIED STRESS AND TEMPERATURE

M.N. Rahaman and L.C. De Jonghe

December 1985

Prepared for the U.S. Department of Energy under Contract DE-AC03-76SF00098

DISCLAIMER

CREEP AND DENSIFICATION DURING SINTERING OF GLASS POWDER COMPACTS: I, EFFECT OF APPLIED STRESS AND TEMPERATURE

M. N. Rahaman and L. C. De Jonghe
Materials and Molecular Research Division
Lawrence Berkeley Laboratory
and
University of California
Berkeley, CA 94720

Abstract

The simultaneous creep and densification of glass powder compacts was studied as a function of applied uniaxial stresses between 0 and 30 kPa and at temperatures between 580°C and 615° C. A strong interaction between creep and densification was observed. This type of interaction has not been found in similar experiments on polycrystalline oxide ceramics. At a fixed temperature, the observed creep rate, $d\varepsilon/dt$, may be expressed as the sum of two terms, i.e. $d\varepsilon/dt = \dot{\rho}\dot{\varepsilon}^{\circ}_{\rho} + \sigma\dot{\varepsilon}^{\circ}_{\sigma}$, where $\dot{\varepsilon}^{\circ}_{\rho}$ and $\dot{\varepsilon}^{\circ}_{\sigma}$ are constants for a particular powder system at fixed temperature, $\dot{\rho}$ is the relative densification rate and σ is the applied stress. For the low stresses used, the volumetric densification rate is almost independent of σ. The effective viscosity for creep, η^{*}_{C}, defined as $1/\dot{\varepsilon}^{\circ}_{\sigma}$ has a strong exponential dependence on porosity, P, and may be expressed as $\eta^{*}_{C} = \exp(-11.2P)$. If the effective viscosities for creep and densification are the same, then the sintering stress, Σ, may be evaluated. Σ reaches a maximum at $\rho \sim 0.82$ then decreases at higher values of ρ. For a constant applied stress, the ratio of the creep rate to the densification rate is independent of temperature. This indicates that both creep and densification in glass powder compacts have the same temperature activation energy.

Supported by the Division of Materials Sciences, Office of Basic Energy Sciences, U.S. Department of Energy, under Contract No. DE-AC03-76SF00098.

I. INTRODUCTION

The early work on the sintering of glass originated from the theory of viscous sintering by Frenkel.[1] Using a simple energy balance, i.e. that the energy dissipated by viscous flow is equal to the energy gained by the reduction of surface area during sintering, Frenkel derived equations for the neck growth between two glass spheres and for the shrinkage of a row of glass spheres. A numerical error in Frenkel's analysis was corrected by Eshelby.[2] The predictions of Frenkel's analysis have been supported by the experimental results of Kuczynski,[3] Kingery and Berg,[4] and Kuczyski and Zaplatynskyj.[5] Using Frenkel's energy balance concept, Mackenzie and Shuttleworth[6] developed a theory for the sintering of glass based on a simple model consisting of isolated, spherical pores of the same size in a dense matrix. Mackenzie and Shuttleworth's analysis is therefore strictly applicable to the final stage of sintering. Experimentally, Cutler and Hendrickson[7] have pointed out the effects of particle shape on the sintering of glass.

Recent work on the sintering of glass is due mainly to Scherer.[8-12] Using Frenkel's energy balance concept, Scherer[8] considered a model that applies to the entire densification process but assumed a particular geometry consisting of cylinders connected into a cubic array. This model clearly does not resemble to microstructure of an actual powder compact but it is believed to provide a reasonable representation of the structure of such materials as flame oxidation performs,[8] phase-separated and leached glasses[9,13] and inorganic

gels.[14] In spite of the peculiar geometry of model, the predicted sintering kinetics agree very well with the predictions of Frenkel's analysis[1] for neck growth between spheres, and with Mackenzie and Shuttleworth's analysis[6] for the sintering of closed, isolated pores. Scherer's model appears therefore to have broad applicability. The model has also been applied to the sintering of a body with a bimodal pore size distribution[11] and to the sintering of a porous glass layer on a rigid substrate.[12] Recently, Rabinovich[15] has compiled a review of the sintering of glass.

The effect of small stresses on the sintering behaviour of glass powder compacts has not been studied before. This paper seeks to address this problem. It describes the simultaneous creep and densification behaviour during the sintering of glass powder compacts using the loading dilatometer technique[16] in which a small, measured, uniaxial stress is applied to the sintering compact. The dependence of the creep rate and the densification rate on applied stress and temperature is explored. A subsequent paper[17] considers the effect of the particle size of the glass powder. In addition to providing a better understanding of sintering and creep phenomena in glass, this work will also be relevant to glass systems in which transient stresses develop during sintering, such as substrates and composites. The loading dilatometer technique has been developed and applied by the present authors to the sintering of polycrystalline oxides, such as CdO[18-20], ZnO[21] and MgO,[22] in which matter transport occurs by diffusion. Comparisons between the glass and the polycrystalline oxide

systems will be pointed out where appropriate.

II. EXPERIMENTAL PROCEDURE

A commercial soda-lime glass powder* was used in this work. The powder was air-classified into narrow size fractions and these were examined using a scanning electron micoscope to determine their average particle sizes. A size fraction with a 4μm average particle size was chosen for these experiments (see Fig. 1(a), Reference 17). The powders were uniaxially pressed at ~20 MPa into cylindrical compacts (6mm diameter by 6mm) with relative densities of 0.55±0.01. About 10 v% of Carbowax** was used as binder.

Compacts were sintered in air for~ 2 to 3 hours in a loading dilatometer.[16] Loads can be held constant to within ±0.5% for the duration of the experiment. Typically, the glass compact was placed in position, and, after the furnace had reached the working temperature, the sample was introduced into the outer zone of the furnace (at ~350 °C) to allow burnout of the binder. After ~30 min, the sample was quickly introduced into the hot zone of the furnace. The load on the compact was applied rapidly and the axial shrinkage and the temperature were recorded continuously. The mass and dimensions of the compacts were measured before and after they were sintered, and the final densities were measured using Archimedes' principle. In a separate set

*Owens-Illinois, Perrysburg, OH 43551

**Union Carbide Corporation, New York, NY 10017

of experiments, sintering was terminated after times between 0 and 3 hours. The dimensions of these compacts were measured using a micrometer and the fracture surfaces were examined using scanning electron microscopy.

Generally, to explore the effects of small applied stresses, experiments were performed at a constant temperature of 605° C and for stresses between 0 and 30 kPa. To study the effect of temperature, experiments were performed at two temperatures, 580° C and 605° C, at an applied stress of 9 kPa.

X-ray diffraction measurements were performed on the glass powder and on the sintered material. For these, the sintered compacts were crushed and ground to a fine powder using a mortar and pestle. CuK_a radiation was used at a scanning rate of 1° 2θ min^{-1}.

The density of the bulk glass was also measured. About 10g of glass powder was placed in a platinum boat and heated to 1300°C at a rate of ~15°C/min, in a nitrogen atmosphere. After ~20 min at this temperature, the sample was slowly cooled to room temperature. The glass sample was then removed and its density measured using Archimedes' principle.

III. RESULTS

The X-ray diffraction results showed no difference in phase compostion between the starting glass powder and the sintered samples.

The complications of phase changes during sintering can therefore be eliminated from the considerations of this work. The density of the bulk glass obtained by melting the gass powder was 2.43±0.01 Mgm^{-3}, and this figure will be used as the theoretical density. Friction between the push rods and the sample led to a small deviation from cylindrical geometry in a narrow region of the sample near its contact surfaces. The diameter near the contact surfaces was slightly larger than that along the rest of the sample. These deviations from cylindrical geometry were small in all experiments and decreased with increasing applied load. The difference between the diameter at the contact surfaces and the average diameter of the sample, obtained from the length of the sample and its density, was less than 3% at the end of any experiment. Frictional effects between the push rods and the sample are therefore relatively insignificant. The effects of applied stress and temperature are now discussed separately in the following sections.

III. (a) EFFECT OF APPLIED STRESS

Fig 1 shows the axial shrinkage, $\Delta L/Lo$, vs time, t, at 605°C for applied loads between 0 and 0.75 N (L_0 = initial sample length and $\Delta L = L-L_0$, where L = instantaneous sample length). A load of 1N represents a stress of 35kPa on the green, unsintered compact and t = 0 represents the beginning of shrinkage. The load was applied quickly at t = 0 and the sintering temperature was reached after t = 8 min. Each curve is the average of two runs under the same conditions and each is

reproducible to within ±2%. It is seen that at any time, t, the axial shrinkage increases with inceasing load.

In these loading dilatometer experiments, the shrinkage of the compact is anisotropic, as shown in Fig. 2 where the axial shrinkage, $\Delta L/L_o$, is plotted vs the radial shrinkage, $\Delta D/D_o$ (D_o = initial sample diameter and $\Delta D = D-D_o$, where D = instantaneous sample diameter). The $\Delta L/L_o$ values are approximately proportional to $\Delta D/D_o$ and the slopes of the lines increase with increasing load.

A key benefit of the loading dilatometer technique is that the creep strain, ε, can be separated from the volumetric strain due to densification. To accomplish this, a methodology described by Raj[23] and the results of Figs. 1 and 2 were used. Fig. 3 shows the relative density, ρ, vs time for zero applied load and for the maximum applied load of 0.75 N. The curves for loads of 0.25 and 0.5 N have been omitted for clarity. Within the limits of experimental error, the small loads cause no change in ρ. Fig. 4 shows the effect of applied load on the creep behaviour. It is seen that the small loads give rise to extensive creep and, at any time, the creep strain, ε, increases with load.

By fitting smooth curves to the results of Figs 3 and 4, and differentiating, the relative densification rate, $d\rho/dt$, and the creep rate, $d\varepsilon/dt$, were obtained as a function of ρ (or t). However, two small corrections have to be included for a more rigorous analysis of these results. First, the cross-sectional area of the compact

decreases during sintering (Fig. 2), causing an increase in the applied stress. Second, the small load applied by the spring of the linear voltage displacement transducer to keep the sample in position, decreases slightly, from 0.1N to zero. This small change in load can be measured as a function of $\Delta L/L_o$ in a separate experiment, using the sensitive load cell in the loading dilatometer. With these corrections, the curves of $d\varepsilon/dt$ vs were evaluated at constant stress, taken as the initial stress on the green compact. A similar correction in $d\rho/dt$ is negligible.

Fig. 5 shows the results for $d\rho/dt$ and $d\varepsilon/dt$ vs ρ at constant applied stresses of 9, 18 and 27 kPa. As noted earlier for ρ, the small applied stresses have almost no effect on $d\rho/dt$. On the other hand, at any ρ, $d\varepsilon/dt$ increases with increasing σ. In fact, a small increase in σ of 18 kPa (from σ = 9 to σ = 27 kPa) causes an increase in $d\varepsilon/dt$ by a factor of ~ 2. Similar to the observations for CdO,[17] it is seen that small uniaxial (or shear) stresses cause extensive shape changes (creep) but have relatively little effect on the volumetric densification rate.

III. (b) EFFECT OF TEMPERATURE

Fig. 6 shows $\Delta L/L_o$ vs time for two temperatures, 580°C and 605°C, under an applied load of 0.25 N. As for many glass systems, it is seen that a small change in temperature causes extensive changes in the shrinkage (or densification). The need for precise temperature control during studies on the sintering of glass is therefore emphasized.

Both $d\rho/dt$ and $d\varepsilon/dt$ at the two temperatures were calculated using the same procedure as that outlined in Section III(a) above. Generally, $d\rho/dt$ and $d\varepsilon/dt$, at any ρ, increase with increasing temperature. The most important result is shown in Fig. 7, where the ratio of the creep rate to the linear densification rate, i.e. $(d\varepsilon/dt)/(1/3\rho)d\rho/dt$ is plotted vs ρ at 580°C and 605°C. It is seen that this ratio is almost independent of temperature. This indicates that both the creep process and the densification process have the same temperature activation energy. Such a finding is quite plausible since it is believed that both creep and densification in glass occur by the same mechanism of viscous flow.

It is worth noting the contrasting effects of uniaxial (or shear) stress and temperature on creep and densification in glass. Creep processes are more easily activated by stress compared to densification processes. On the other hand, temperature activates both processes equally. Therefore, temperature cannot be used to vary the ratio $d\varepsilon/dt$ to $d\rho/dt$. To accomplish this, applied stress and/or particle size[17] of the powder should be changed.

IV. DISCUSSION

To explore the functional dependence of $d\varepsilon/dt$ on σ, the results of Fig. 5 may be replotted as $d\varepsilon/dt$ vs σ at different values of ρ. This is shown in Fig. 8. It is seen that $d\varepsilon/dt$ increases linearly with σ, in agreement with the predicted stress dependence for a Newtonian viscous flow mechanism. A remarkable aspect of the creep data is that

they extrapolate to a significant total creep rate at zero applied stress. This extrapolated creep rate depends on the compact density. In fact, if the extrapolated creep rate is plotted against the relative densification rate, $\rho(=d\rho/dt)$, a linear proportionality is evident, Fig. 9. Thus, at applied stresses above 10 kPa, the observed creep rate can be written as

$$d\varepsilon/dt = \dot{\rho}\dot{\varepsilon}^{\circ}_{\rho} + \sigma\dot{\varepsilon}^{\circ}_{\sigma} \qquad \text{Eqn. 1}$$

where $\varepsilon^{\circ}_{\rho}$ and $\varepsilon^{\circ}_{\sigma}$ are constants for a particular powder system at a fixed temperature. This equation clearly can not hold as the applied stress approaches zero and implies a strong non-linear relation between the creep rate and applied stress for stresses much lower than those used in these experiments. It must therefore be concluded that there is considerable interaction between the densification process and the creep process during the sintering of glass. This type of interaction has not been observed in the creep-sintering of polycrystalline oxide ceramics,[18] for which the creep strains are somewhat smaller than those reported here.

As a consequence of the interaction between creep and densification, we should also write

$$d\rho/dt = \dot{\rho}(\Sigma) = + \dot{\rho}(\sigma) \qquad \text{Eqn. 2}$$

where $\rho(\Sigma)$ and $\rho(\sigma)$ represent the contributions to $d\rho/dt$ from the sintering stress, Σ, and from σ, respectively. The sintering stress is equal to γK, where γ is the surface tension and K is the average

curvature of the pore surfaces. For the glass powder used, $\dot{\rho}(\sigma)$ is not observed because the equivalent hydrostatic stress due to σ, i.e. $\sigma/3$ is much less than Σ. Further considerations regarding the interaction between the creep and densification processes in glass are contained in a subsequent paper.[17]

Both $\dot{\varepsilon}^{\circ}_{\rho}$ and $\dot{\varepsilon}^{\circ}_{\sigma}$ were found from Fig. 8 by using a simple least-squares fitting technique. Fig. 10 shows the component of the creep rate due to applied stress, i.e. $\sigma\dot{\varepsilon}^{\circ}_{\sigma}$, vs porosity, P (= 1-$\rho$), for σ = 9 kPa. Now, the effective viscosity, η^{*}_{c}, for creep of the glass compact is defined as

$$\eta^{*}_{c} = \sigma/(\sigma\dot{\varepsilon}^{\circ}_{\sigma}) = 1/\dot{\varepsilon}^{\circ}_{\sigma} \qquad \text{Eqn. 3}$$

The results of Fig 10 show that η^{*}_{c} has a strong exponential dependence on P (or ρ) i.e. $\eta^{*}_{c} = \eta^{\circ} \exp(-aP)$, where a = 11.2±0.2, and η° is the viscosity of the bulk glass. It should be pointed out that only $\sigma\dot{\varepsilon}^{\circ}_{\sigma}$ and not $d\varepsilon/dt$ should be used in Eqn. 3, since the total creep rate, $d\varepsilon/dt$, contains a significant contribution from the densification process. η° was found by extrapolating the data of Fig. 9 to zero porosity, yielding $\eta^{\circ} = (1.3 \pm 0.1) \times 10^{10}$ $Nm^{-2}S$.

By analogy to the creep process, the linear densification rate may be written as

$$(1/3\rho)\, d\rho/dt = \Sigma/\eta^{*}_{d} \qquad \text{Eqn. 4}$$

where Σ is the sintering stress and η_d^* is the effective viscosity for the densification process. Since both creep and densification occur by the same mechanism, it may be reasonably assumed that $\eta_c^* = \eta_d^*$. With this assumption, then

$$\Sigma = (d\rho/dt)/(\dot{\varepsilon}_\sigma^\circ 3\rho) \qquad \text{Eqn. 5}$$

Σ can then be calculated as a function of ρ, and the results are shown in Fig. 11. It is seen that Σ reaches a maximum at $\rho \sim 0.82$. An explanation of the decrease in Σ at higher ρ may lie in the elaborate pore microstructure as shown in Fig. 12(a) for a compact sintered to $\rho \sim 0.8$. Collapse of the elongated pores as the microstructure moves from the interconnected to the closed pore situtation may give rise to this decrease in Σ above $\rho \sim 0.82$. The variation of Σ with ρ for glass is markedly different from that for polycrystalline CdO,[19] where extensive grain (pore) growth causes Σ to decrease slightly with inceasing ρ. As shown in Fig. 12(b), for a compact sintered to $\rho \sim 0.85$, the pore microstructure in CdO is much more rounded.

Regardless of the actual variation of Σ with ρ, it is seen that Σ lies in the range 140 to 180 kPa during the experiment. The negligible effect of σ on $d\rho/dt$ is now clear since the equivalent applied hydrostatic stress, equal to $\sigma/3$, is only 9 kPa even for the maximum stress used.

CONCLUSIONS

The application of the loading dilatometer technique to study the simultaneous creep and densification behaviour of glass powder compacts has led to the observation of extensive interaction between the creep and densification processes. This is the first time that such an interaction has been observed.

The observed total creep rate, $d\varepsilon/dt$, can be expressed as the sum of two terms, i.e. $d\varepsilon/dt = \dot{\rho}\dot{\varepsilon}^{\circ}_{\rho} + \sigma\dot{\varepsilon}^{\circ}_{\sigma}$, where $\dot{\rho}\dot{\varepsilon}^{\circ}_{\rho}$ represents the contribution from the densification process and $\sigma\dot{\varepsilon}^{\circ}_{\sigma}$ is a linear function of the applied stress, σ.

The effective viscosity for creep, η^{*}_{c}, defined as the ratio $\sigma/(\sigma\dot{\varepsilon}^{\circ}_{\sigma})$ has a strong exponential dependence on porosity, P, and can be expressed as $\eta^{*}_{c} = \exp(-11.2P)$. The bulk viscosity of the glass is 1.3×10^{10} $Nm^{-2}S$.

The assumption that the effective viscosities for creep and densification are the same leads to the measurement of the sintering stress, Σ. It is found that Σ inceases to a maximum at $\rho \sim 0.82$, then decreases at higher ρ. The magnitude of Σ is in the region of 140-180 kPa for $0.65 < \rho < 0.9$.

The ratio of the creep rate to the densification rate is independent of temperature, indicating that both creep and densification in glass have the same temperature activation energy.

ACKNOWLEDGMENT:

The authors wish to thank R. J. Brook and R. M. Cannon for very helpful discussions.

REFERENCES

1. J. Frenkel,"Viscous Flow of Crystalline Bodies Under the Action of Surface Tension", J. Phys. (Moscow) **9** (5) 385-91 (1945).

2. J. D. Eshelby in Discussion of "Seminar on the Kinetics of Sintering" by A. J. Shaler, Metals Trans., **185** 806, November 1949.

3. G. C. Kuzcynski, "Study of the Sintering of Glass" J. Appl. Phys. **20** (12) 1160-63 (1949).

4. W. D. Kingery and M. Berg, "Study of the Initial Stages of Sintering Solids by Viscous Flow, Evaporation-Condensation, and Self-Diffusion", J. Appl. Phys. **26** (10) 1205-12 (1955).

5. G. C. Kuzcynski and I. Zaplatynskyj, "Sintering of Glass", J. Amer. Ceram. Soc. **39** (10) 349-50 (1956).

6. J. K. Mackenzie and R. Shuttleworth, "A Phenomenological Theory of Sintering", Proc Phys Soc, London, **62** (12B) 833-52 (1949).

7. I. B. Cutler and R. E. Hendricksen, "Effect of Particle Shape on the Kinetics of Sintering of Glass", J. Am. Ceram. Soc. **51** (10) 604-5 (1968).

8. G. W. Scherer, "Sintering of Low-Density Glasses: I, Theory", J. Am. Ceram. Soc **60** (5-6) 239-43 (1977).

9. G. W. Scherer and D. L. Bachman, "Sintering of Low-Density Glasses: II, Experimental Study" J. Am. Ceram. Soc., **60** (5-6) 239-43 (1977).

10. G. W. Scherer, "Sintering of Low-Density Glasses: III, Effect of a Distribution of Pore Sizes", J. Am. Ceram. Soc., **60** (5-6) 243-46 (1977).

11. G. W. Scherer, "Viscous Sintering of a Bimodal Pore-Size Distribution", J. Am. Ceram. Soc. **67** (11) 709-15 (1984).

12. G. W. Scherer and T. Garino, "Viscous Sintering on a Rigid Substrate", J. Am. Ceram. Soc. **68** (4) 216-20 (1985).

13. G W. Scherer and M. G. Drexhage, "Stress in Leached Phase-Separated Glass", J. Am. Ceram. Soc. **68** (8) 419-26 (1985).

14. C. J. Brinker and G. W. Scherer, "Relationships Between the Sol-to-Gel and Gel-to Glass Conversions", pp. 43-59 in Ultrastructure Processing of Ceramics, Glasses and Composites. L. L. Hench and D. R. Ulrich (Ed:) Wiley, New York (1984).

15. E. M. Rabinovich, "Preparation of Glass by Sintering", J. Mater Sci., 20 (11) 4259-4297 (1985).

16. L. C. De Jonghe and M. N. Rahaman, "A Loading Dilatometer" Rev Sci. Instrum., **55** (12) 2007-10 (1984).

17. M. N. Rahaman, L. C. De Jonghe and R. J. Brook, "Creep and Densification During Sintering of Glass Powder Compacts: II, Effect of Particle Size" following article.

18. M. N. Rahaman and L. C. De Jonghe "Sintering of CdO Under Low Applied Stress", J. Am. Ceram. Soc., **67** (10) C-205-7 (1984).

19. M. N. Rahaman, L. C. De Jonghe and R. J. Brook, "Effect of Shear Stress on Sintering", J. Am. Ceram. Soc., January, 1986.

20. M. N. Rahaman, L. C. De Jonghe and C. H. Hseuh, "Creep During Sintering of Porous Compacts", J. Am. Ceram. Soc. January, 1986.

21. M. N. Rahaman and L. C. De Jonghe, "Creep and Densification of Zinc Oxide", unpublished work.

22. M. Lin, M. N. Rahaman and L. C. De Jonghe, "Sintering and Creep of MgO Powder Compacts", for abstract see Am. Ceram Soc. Bull. 64 (9) 219 (1985).

23. R. Raj, "Separation of Cavitation-Strain and Creep-Strain During Deformation", J. Am. Ceram. Soc., **65** (3) C-46 (1982).

LIST OF FIGURES

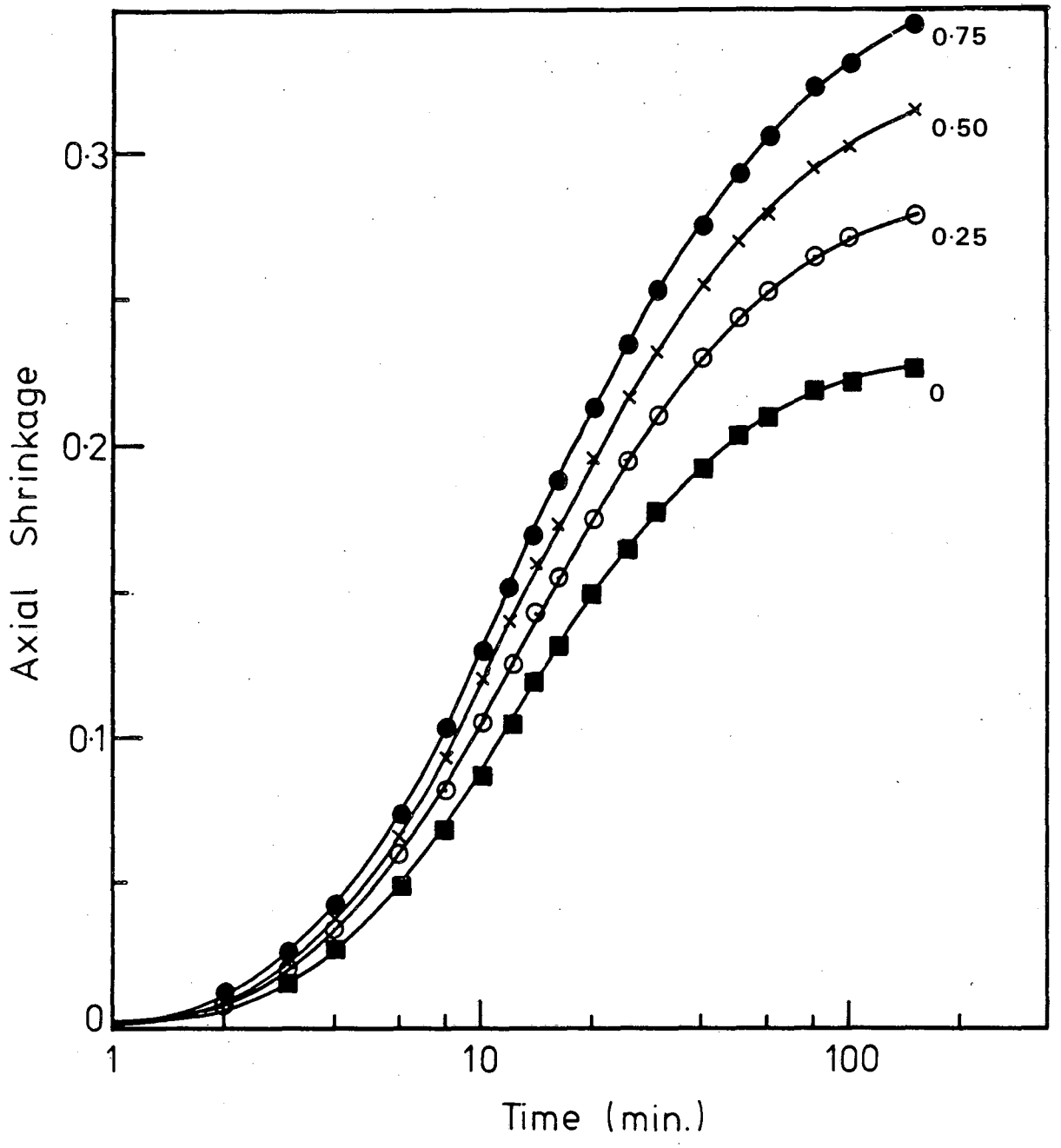

XBL 862-493

I: Fig. 1

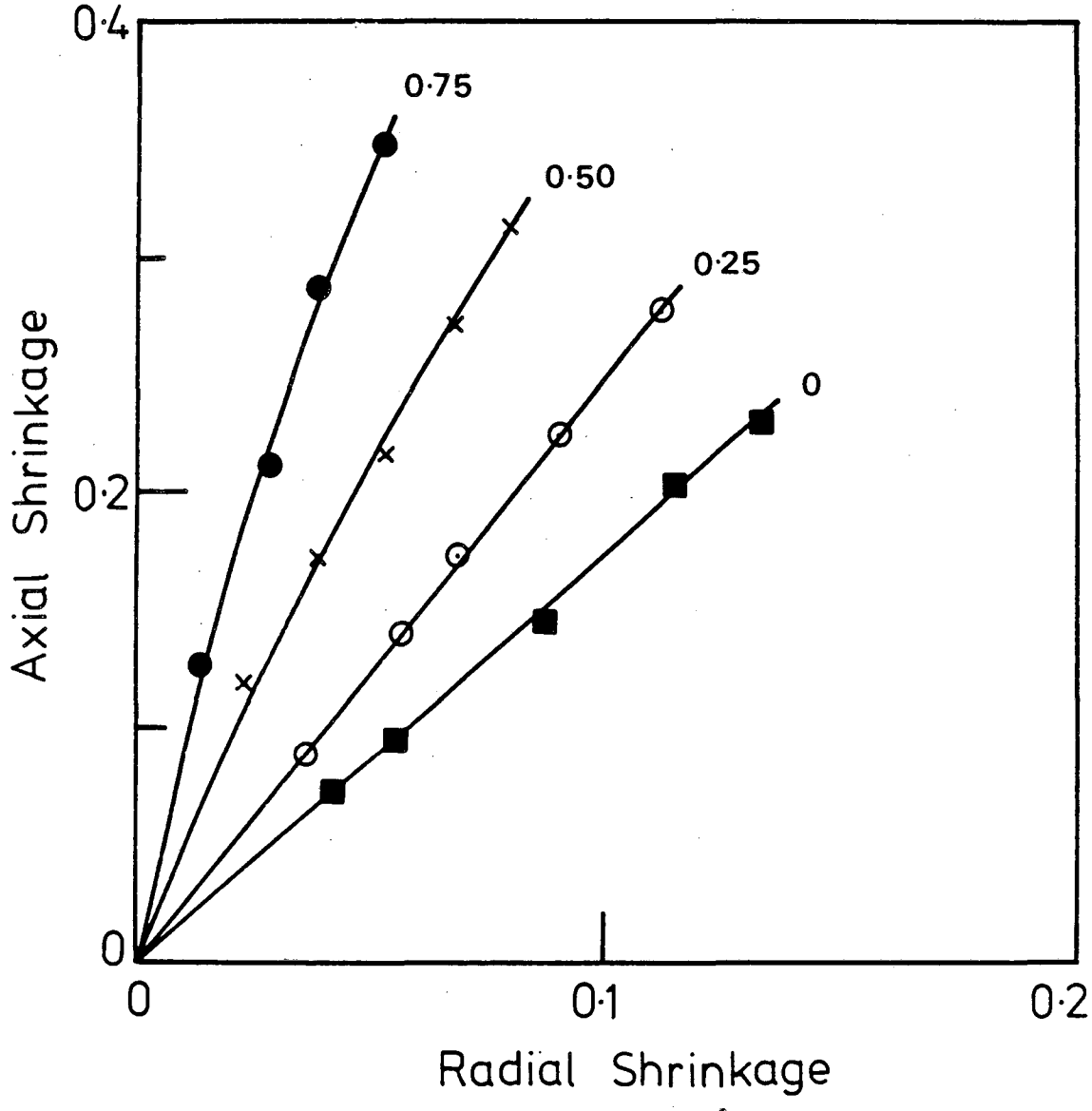

XBL 862-492

I: Fig. 2

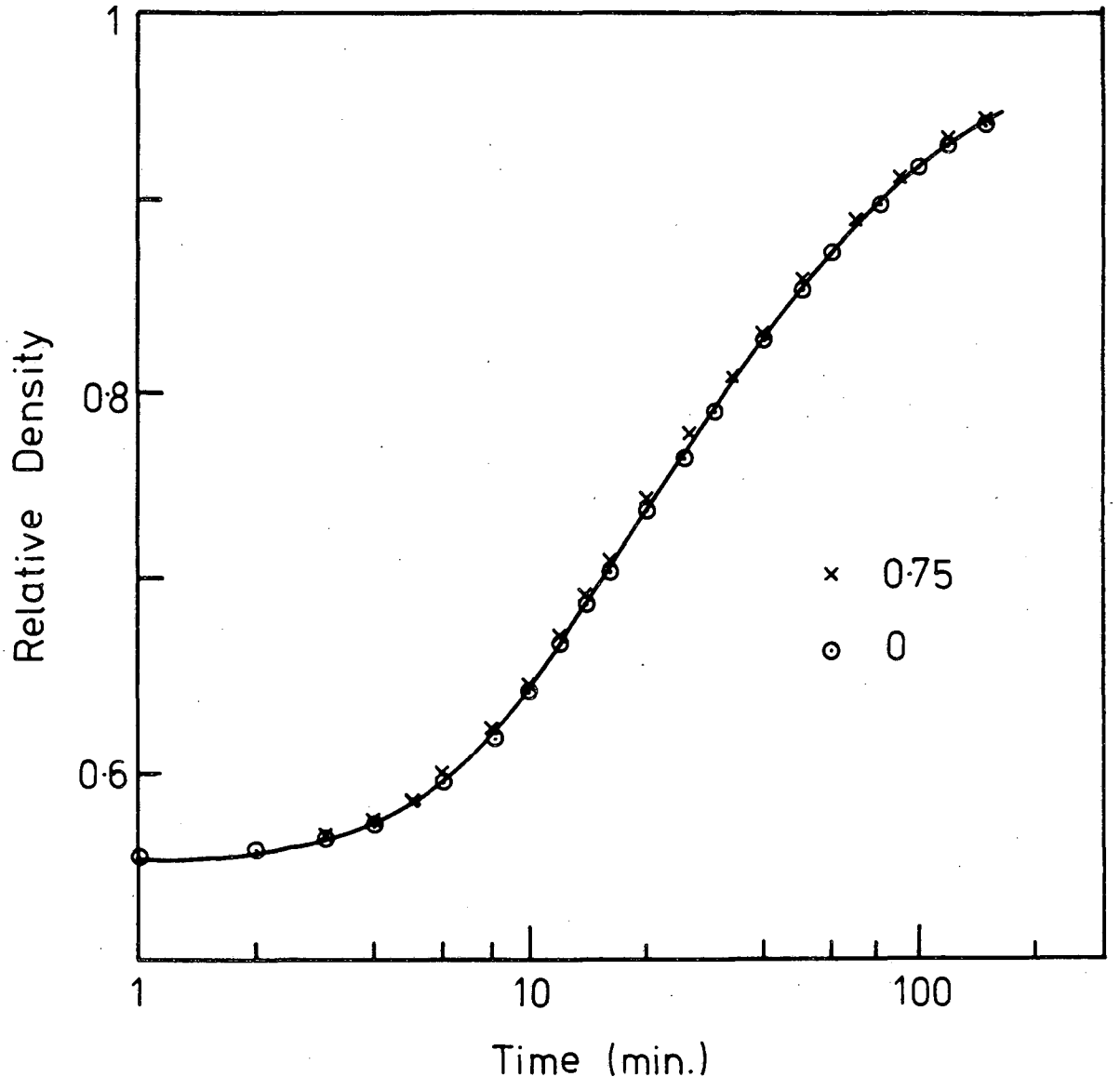

XBL 8510-4442

I: Fig. 3

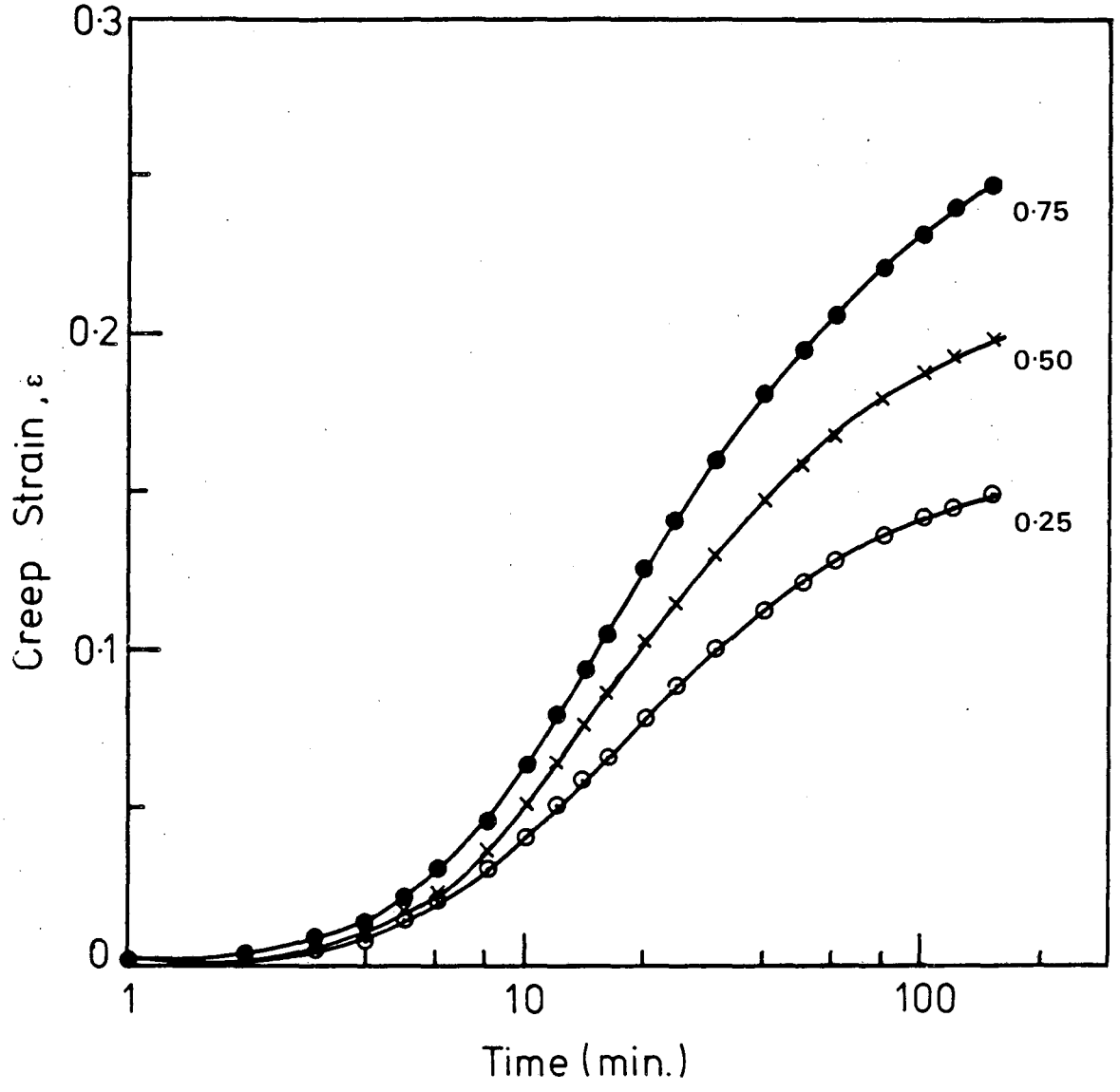

XBL 8510-4441

I: Fig. 4

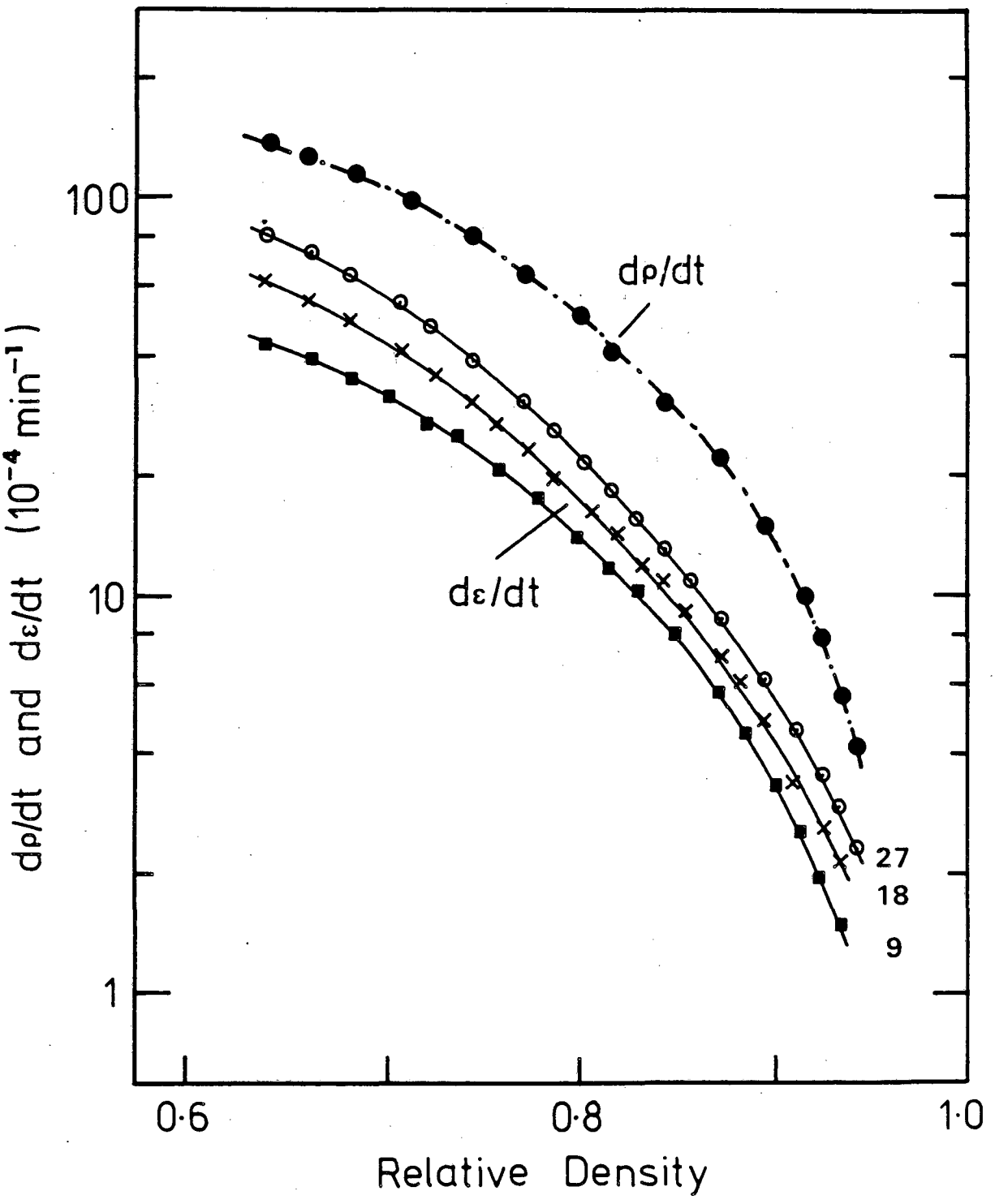

XBL 8510-4440

I: Fig. 5

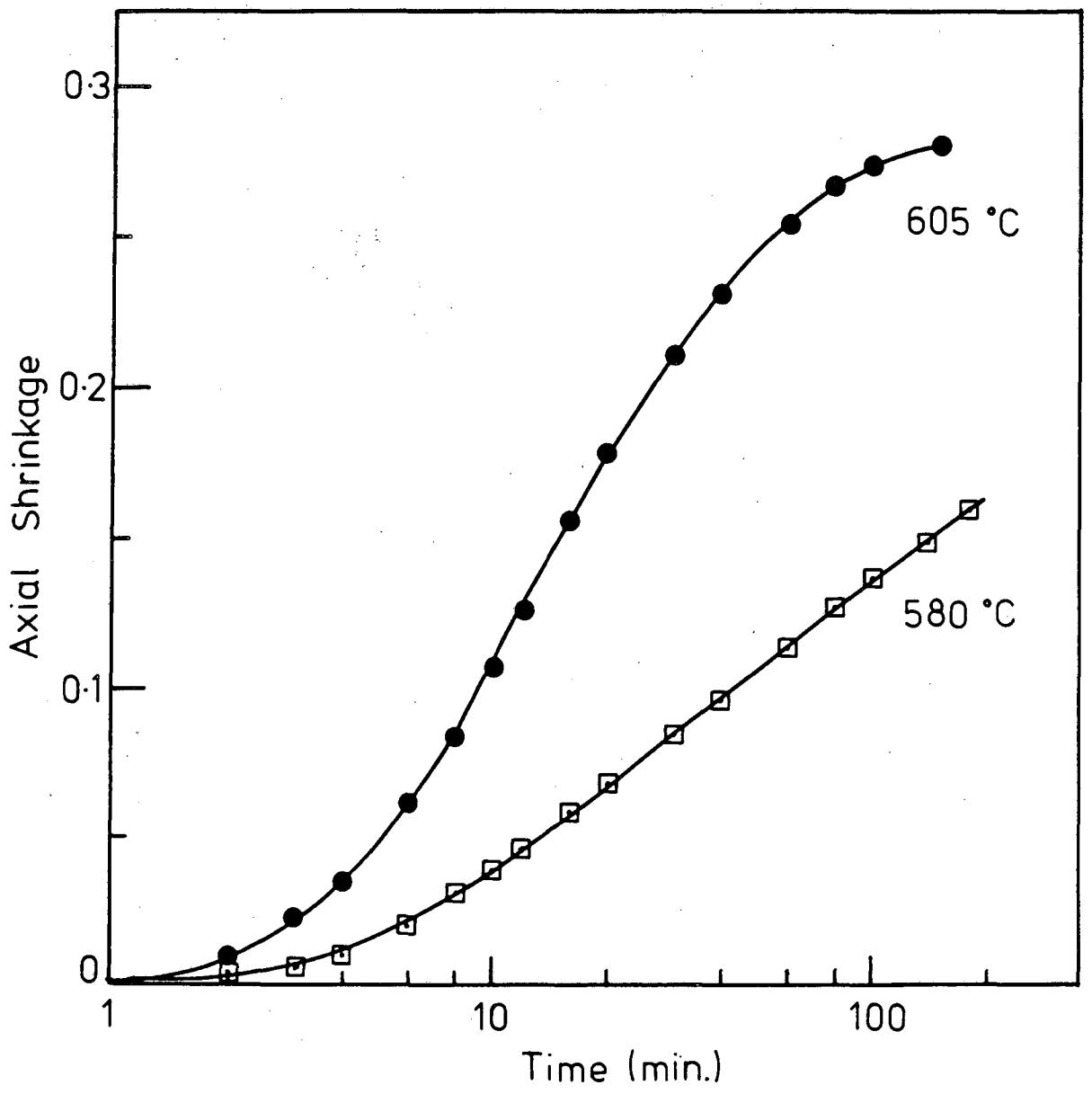

XBL 862-491

I: Fig. 6

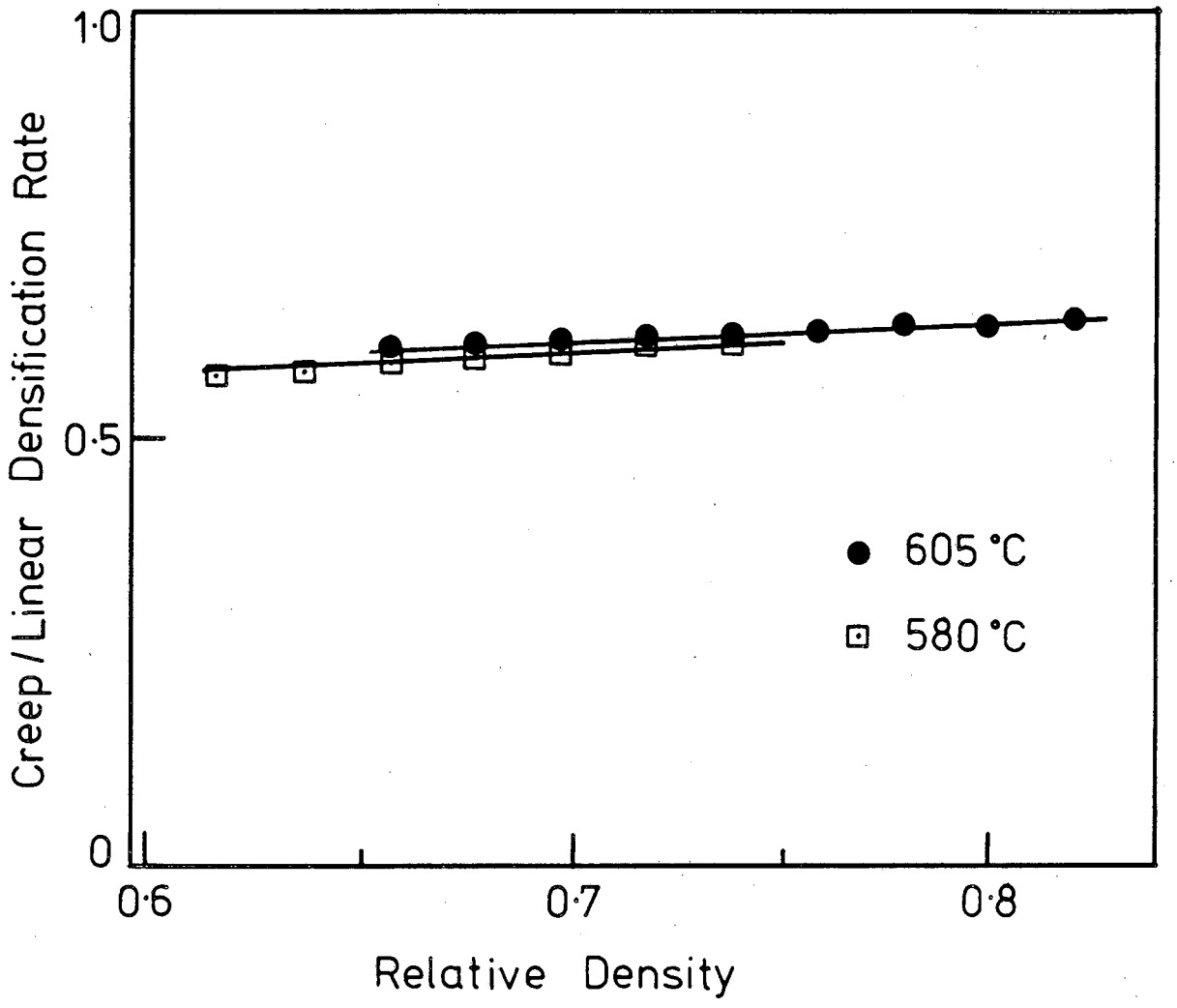

XBL 8510-4446

I: Fig. 7

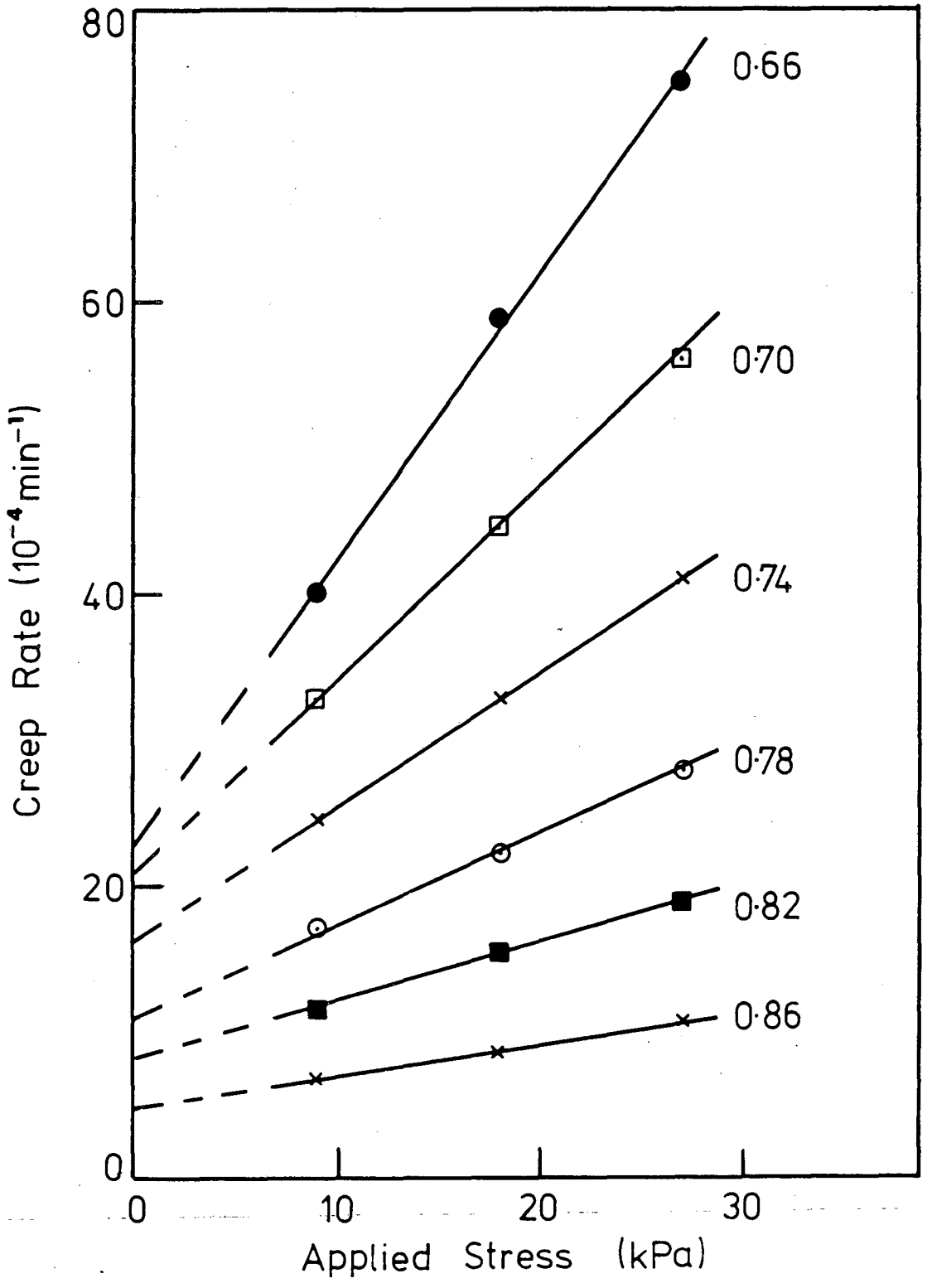

XBL 8510-4447

I: Fig. 8

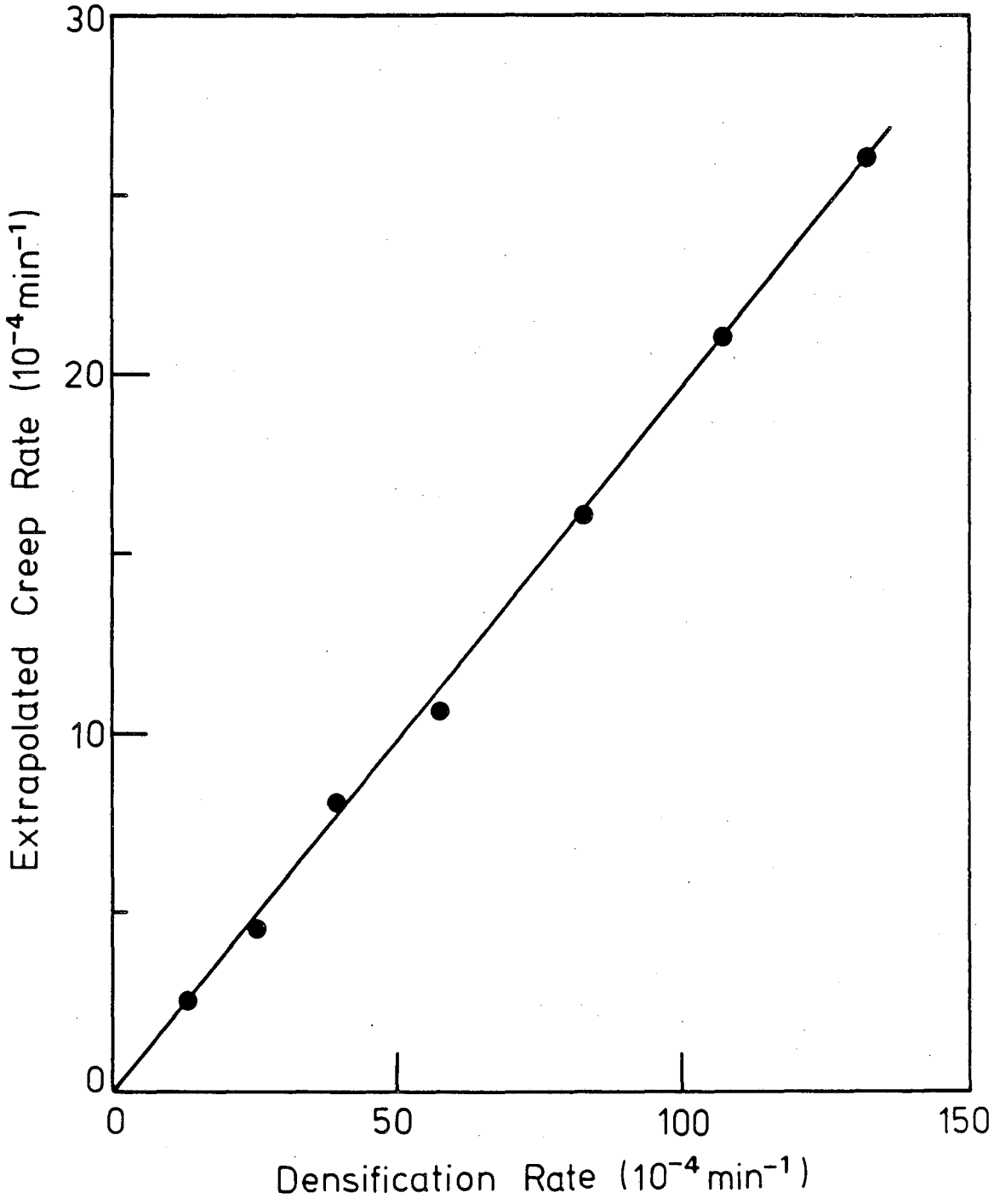

XBL 862-490

I: Fig. 9

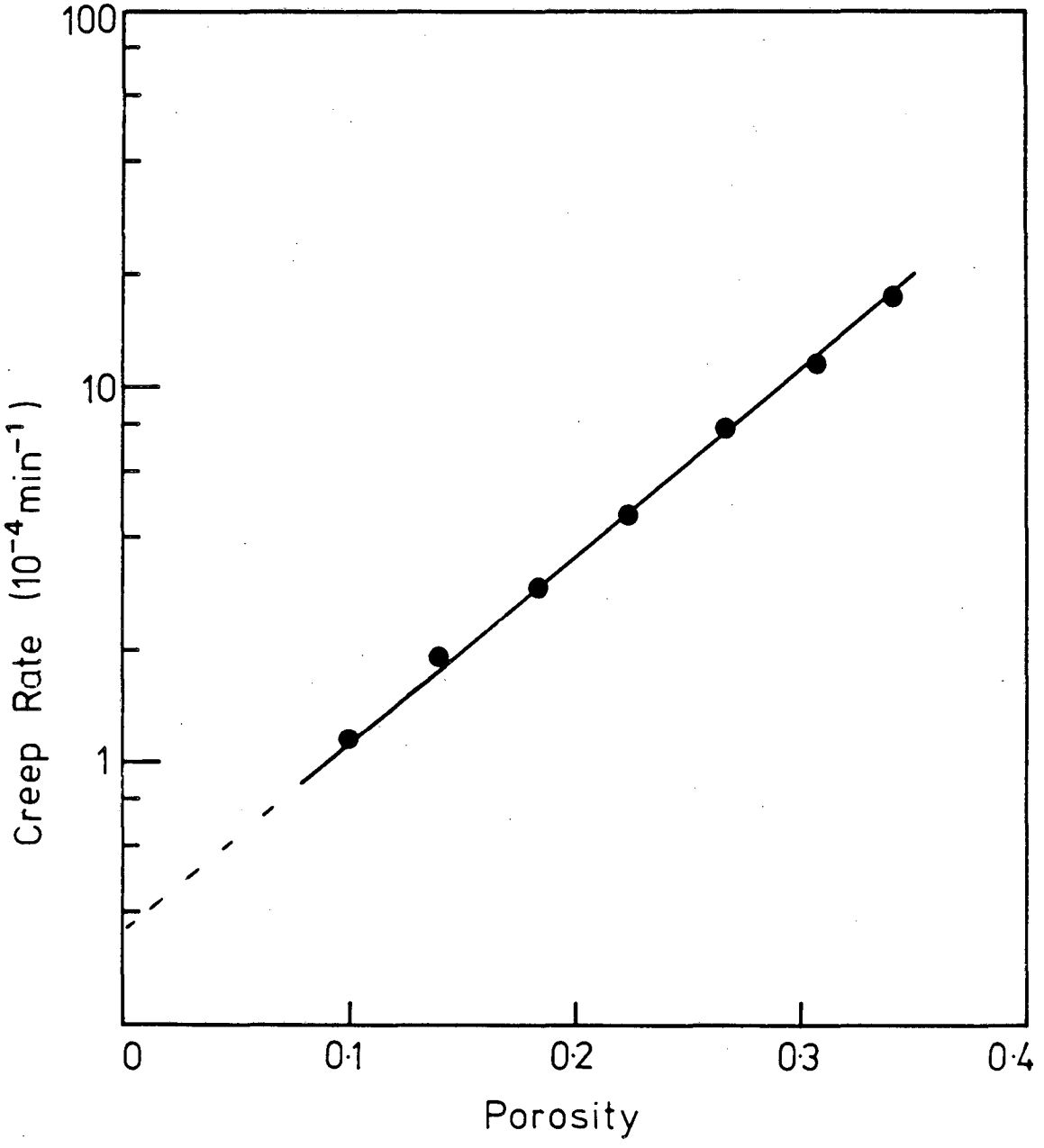

XBL 8510-4434

I: Fig. 10

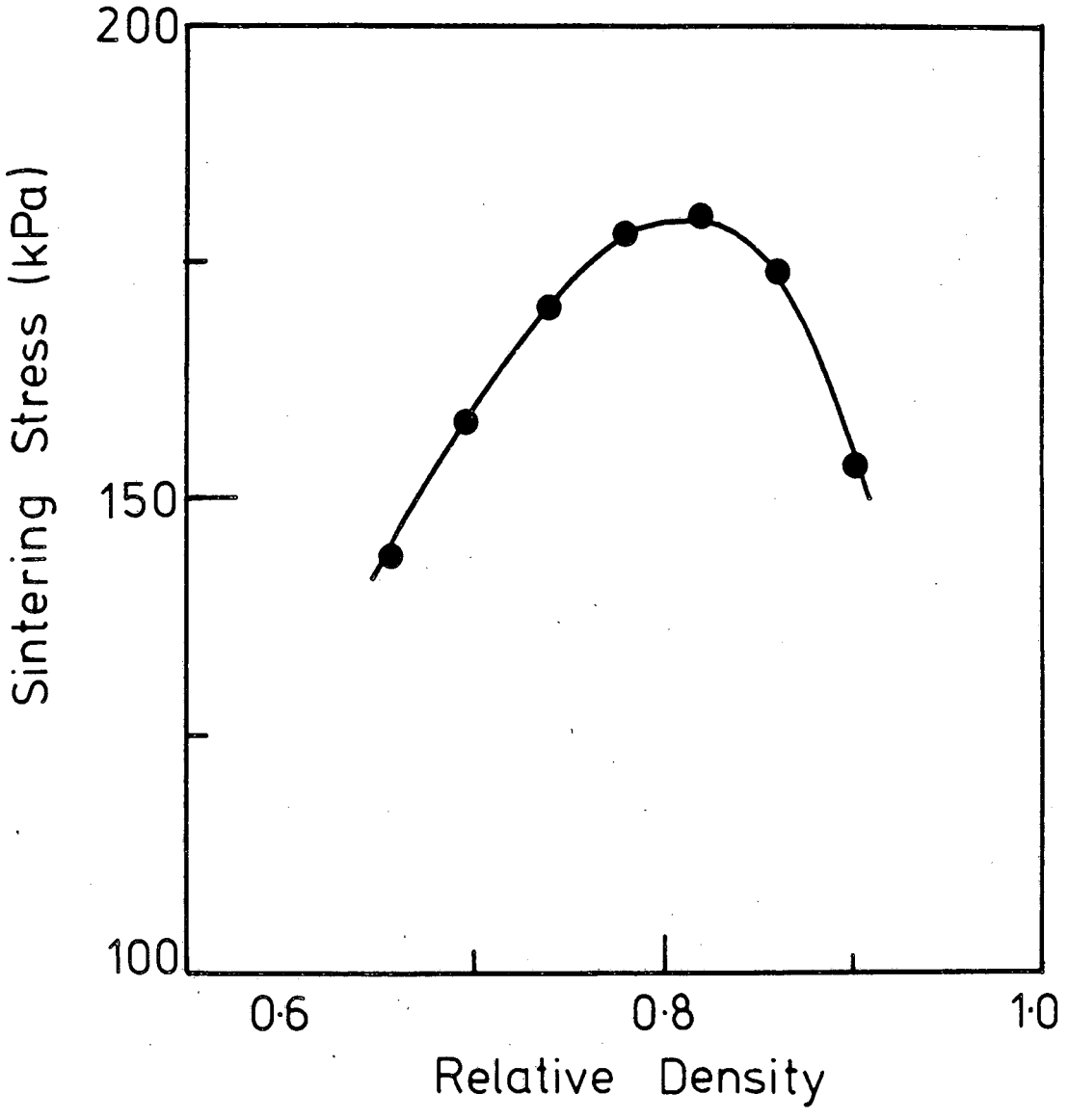

XBL 862-489

I: Fig. 11

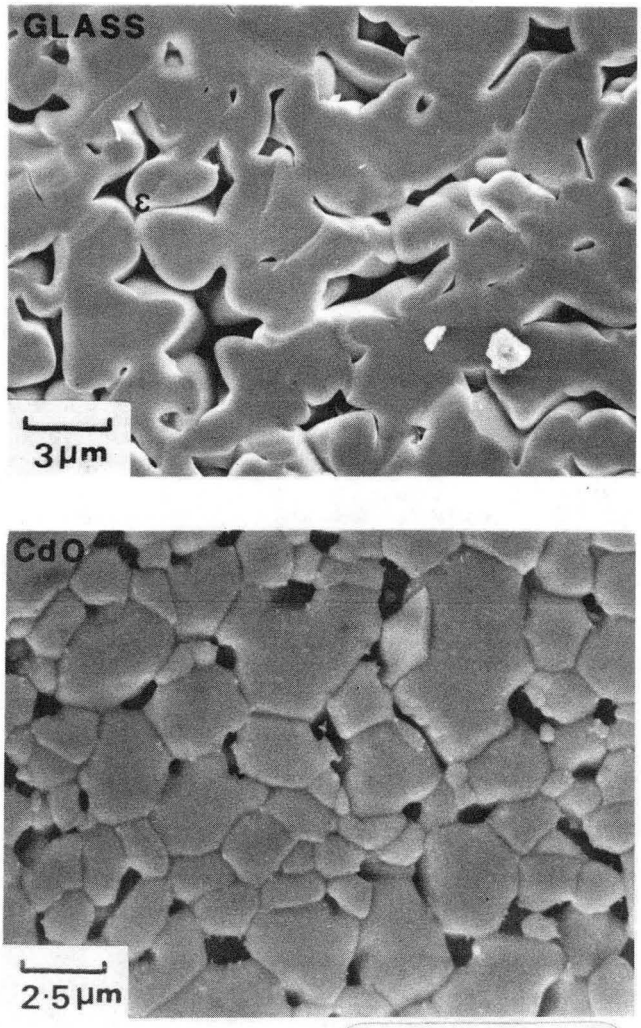

XBB 857-5478A

I: Fig. 12

This report was done with support from the Department of Energy. Any conclusions or opinions expressed in this report represent solely those of the author(s) and not necessarily those of The Regents of the University of California, the Lawrence Berkeley Laboratory or the Department of Energy.

Reference to a company or product name does not imply approval or recommendation of the product by the University of California or the U.S. Department of Energy to the exclusion of others that may be suitable.

LAWRENCE BERKELEY LABORATORY
TECHNICAL INFORMATION DEPARTMENT
UNIVERSITY OF CALIFORNIA
BERKELEY, CALIFORNIA 94720